IEEE Photonics Journal
An IEEE Photonics Society Publication

Open Access

Coupled-Ring-Resonator-Mirror-Based Heterogeneous III–V Silicon Tunable Laser

Volume 7, Number 3, June 2015

S. Srinivasan
M. Davenport
T. Komljenovic
J. Hulme
D. T. Spencer
J. E. Bowers, Fellow, IEEE

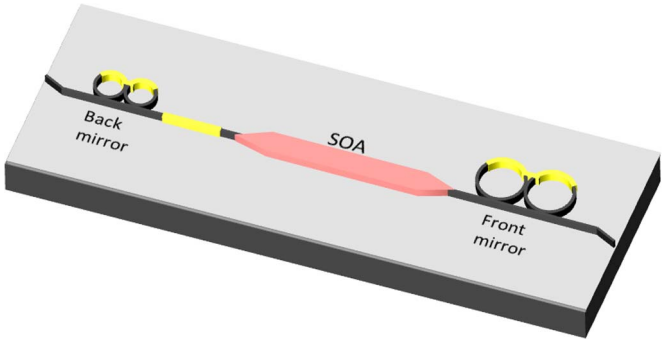

DOI: 10.1109/JPHOT.2015.2428255
1943-0655 © 2015 IEEE

IEEE photonics SOCIETY

IEEE

Coupled-Ring-Resonator-Mirror-Based Heterogeneous III–V Silicon Tunable Laser

S. Srinivasan, M. Davenport, T. Komljenovic, J. Hulme, D. T. Spencer, and J. E. Bowers, *Fellow, IEEE*

Department of Electrical and Computer Engineering, University of California, Santa Barbara, CA 93106 USA

DOI: 10.1109/JPHOT.2015.2428255
1943-0655 © 2015 IEEE. Translations and content mining are permitted for academic research only. Personal use is also permitted, but republication/redistribution requires IEEE permission. See http://www.ieee.org/publications_standards/publications/rights/index.html for more information.

Manuscript received February 6, 2015; revised April 21, 2015; accepted April 23, 2015. Date of current version May 26, 2015. This work was supported by the DARPA EPHI Program. The work of T. Komljenovic was supported by NEWFELPRO under Grant 25. Corresponding author: S. Srinivasan (e-mail: sudharsanan87@gmail.com).

Abstract: We show theoretical and experimental results from a tunable laser, with its center wavelength in the C-band, designed using coupled-ring resonator mirrors. The effective cavity length enhancement and negative optical feedback obtained from the resonators helps to narrow the laser linewidth in a small form factor. We report a linewidth of 160 kHz and a side-mode suppression ratio of > 40 dB over the full tuning range.

Index Terms: Tunable lasers, coupled resonators, semiconductor lasers, silicon photonics.

1. Introduction

Significant savings in cost, power and space are possible in existing optical data transmission networks through photonic integration. Photonic integration can be broadly classified into two categories, hybrid and monolithic integration. The former involves assembling multiple single functionality optical devices together into a single package including any optical coupling and/or electronic connections. A very good laser demonstration using hybrid integration was reported in [1]. On the other hand monolithic integration assembles many devices or optical functionalities on a single chip so that all the optical connections are on chip and require no external alignment. This provides a substantial improvement in reliability and simplifies testing. Monolithic integration has been demonstrated on both indium phosphide (InP) and silicon (Si) substrates. An example of high density integration on InP was shown by Infinera [2] and shows the viability of integrating a 1 Tbps coherent transmitter on a single chip in the near future. Integration on larger 300 mm Si substrates can further bring down the cost and has been a major area of research in recent years. Heterogeneously integrating III–V materials on silicon also improves the individual device performance, mainly due to lower propagation losses and better lithography.

A key requirement for better spectral efficiency in a coherent optical link is to use a monolithically integrated narrow linewidth laser. For example, a 16 quadrature amplitude modulation format requires a laser linewidth < 300 kHz [3]. The laser also needs to be tunable to align to a certain ITU grid and to aid or replace an existing channel. This poses a unique challenge of designing a tunable and narrow linewidth laser. There have been several results prior to this work addressing this need [4]–[7]. This paper summarizes results from a tunable laser using coupled

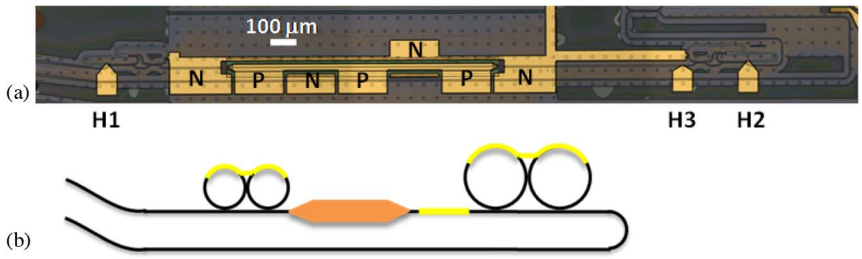

Fig. 1. (a) Microscope image of the hybrid silicon laser. (b) Schematic of the laser showing the design using CRR mirrors. Wavelength tuning is achieved by thermally tuning the waveguides (black lines) underneath the tuners (yellow lines). The orange section is the SOA for gain. P—laser anode; N—laser cathode; H1, H2, H3—positive terminal for each heater pads. The negative terminal of all heaters is shorted to laser cathode.

ring resonator (CRR) mirrors that has high output power ($>$ 15 mW) and low linewidth (160 kHz) by exploiting the effective cavity length enhancement and negative optical feedback from the ring resonators. This paper is organized as follows: Section 2 covers the details of the laser design followed by the results in Section 3. We discuss certain important design considerations for CRR mirrors in Section 4 and then conclude.

2. Laser Design and Fabrication

The advantage of using ring resonators, as opposed to Bragg gratings, in a tunable laser was first shown by Liu *et al.* [8]. The resonance enhancement of cavity length together with the Vernier effect can simultaneously provide a narrow linewidth and a wide tuning range. Traditional mirror designs using ring resonators usually have unwanted ports through which useful laser light is left untapped [1], [4]–[7]. The advantage of using a CRR mirror design is that we avoid having a drop port bus waveguide to form the necessary filter shape and have a simple two output-port laser. One or more of the directional couplers in a CRR mirror can be made 100% to produce light in a single direction. The microscope image and a schematic of the fabricated laser are shown in Fig. 1.

The laser cavity is formed by two coupled ring resonator pairs on either side of the semiconductor optical amplifier (SOA). Each pair has a particular circumference that modulates the mirror loss spectrum to provide a unique wavelength where the reflectivity is high. Tuning is achieved by heating each mirror to control the lasing wavelength. The 78 nm thick heater metal comprises of alternating layers of 12 nm Nickel and 6 nm Chromium and is deposited on 1 μm silicon dioxide spacer above the silicon waveguide to reduce losses. The heater metal is 10 μm wide and has a resistance of 1 kΩ/mm. The circumferences chosen for each pair are 471 μm and 513 μm, respectively. These lengths were limited by the directional coupler lengths and the minimum bend radius. The waveguides at the resonators were fully etched to minimize process variations in etch depth. The top silicon thickness of the SOI is 500 nm, and the waveguide width is 400 nm to keep the bend radius small and for single mode operation. Fig. 2 shows scanning electron microscope (SEM) images of the directional coupler section used in the CRR mirrors and the waveguide sidewall as examples of good silicon process control. The waveguide width tapers out to 950 nm under the SOA. The length of the SOA is 1040 μm including the tapers. The active region comprises of 7 InGaAlAs quantum wells [9]. The output waveguides on both sides taper out to a waveguide width of 5 μm and terminate at the facet at an angle of 7° to minimize reflections.

The design of the CRR mirror as a filter and as a reflector for lasers has been studied extensively by many authors [10]–[12]. The CRR mirror can provide various filter shapes with multiple resonances after each free spectral range (FSR). However, for a reflector in a tunable laser design we chose the coupling strengths that were required to achieve a single resonance peak. Fig. 3(a) shows a CRR mirror with labels for power coupling coefficient for the three couplers. In our design we have $\kappa_1 = \kappa_2 = 2.25\%$ and $\kappa_3 = 36\%$, at the center wavelength

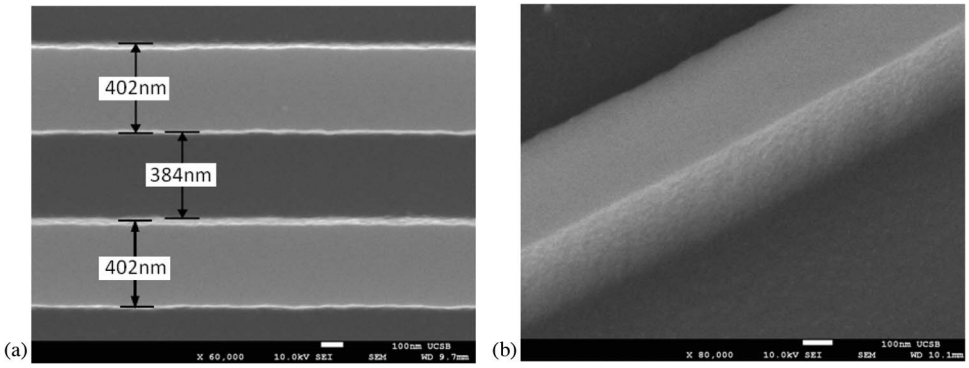

Fig. 2. SEM images showing (a) directional coupler gap, designed for 400 nm waveguide width and 400 nm gap, and (b) waveguide isometric view with a smooth vertical sidewall.

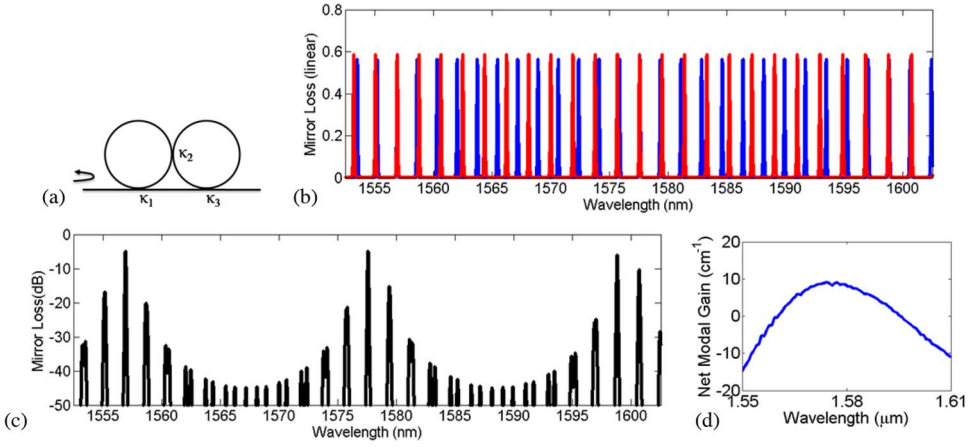

Fig. 3. (a) CRR mirror schematic. Reflection spectrum of each CRR mirror (b) and the composite mirror loss spectrum (c) of the laser cavity. (d) Net modal gain $(\Gamma g - \langle \alpha_i \rangle)$ of a 1 mm long SOA, where Γ is the confinement factor, g is the material gain, and $\langle \alpha_i \rangle$ is the internal loss per unit length.

of 1575 nm. The simulated suppression ratio of the interstitial peaks is $>$ 12 dB for the chosen design, which should be more than sufficient to suppress the longitudinal modes by $>$ 40 dB. The gap width is critical to the coupling strength and we rely on the DUV lithography system to achieve this within 5% of the desired value. The stronger coupler (κ_3) is fairly robust to coupling variations, by as much as $\pm$5%. However, the weaker coupler (κ_1, κ_2) is quite sensitive and needs to be precise to achieve the desired mirror response. However, the slope of the curve between coupling strength and coupler length is quite small for small coupler lengths and was useful in achieving the target reflectivity despite gap variations. The strength of the directional coupler increases with increasing wavelength. In the tuning range of 30 nm, the coupling strength variations influence the mirror loss but the laser maintains single mode operation. This is because the interstitial peaks in the mirror loss spectrum are well suppressed at the optimum design value and any variation in coupling from changing wavelength still keeps the interstitial peaks suppressed enough to achieve single mode operation. The reflection spectrum of each CRR mirror and the composite spectrum are shown in Fig. 3(b) and (c) for a waveguide loss of 5 dB/cm. The output spectrum is not influenced by the relative distance between couplers within the CRR mirror. Fig. 3(d) shows the net modal gain of a 1.1 mm long SOA with tapers extracted from spectral measurements as a function of input current density. These measurements were done on independent Fabry–Perot lasers on the same die.

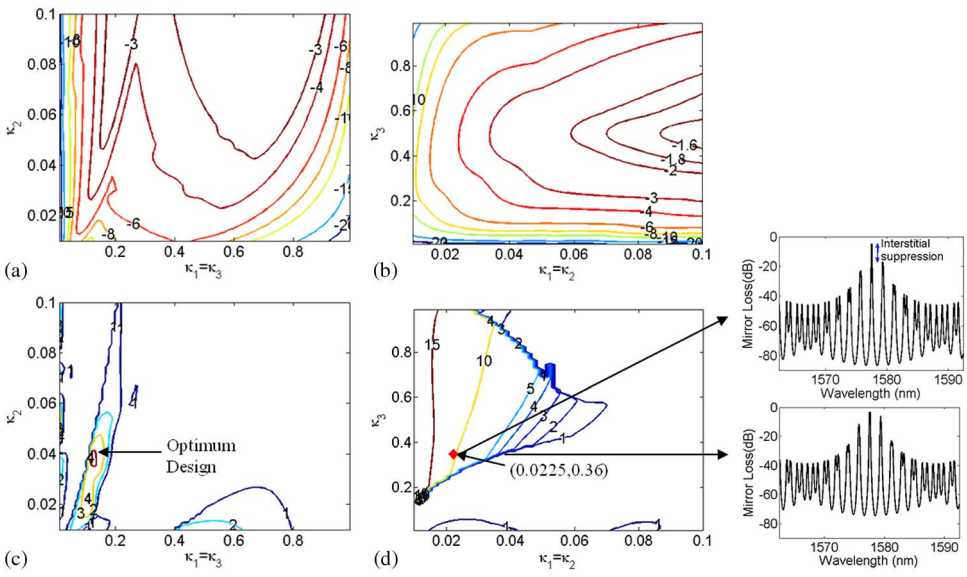

Fig. 4. Mirror loss and interstitial peak suppression ratio (in dB) for the traditional symmetric CRR design (a), (c) and asymmetric design (b), (d) for various values of coupling efficiency $\kappa_1, \kappa_2, \kappa_3$, respectively. The waveguide loss assumed is 1 cm^{-1}. (Inset) Mirror loss spectrum showing the interstitial suppression for two sets of coupling coefficients.

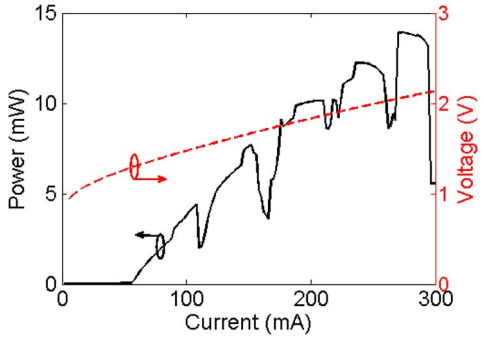

Fig. 5. LIV curve for the tunable laser at 20 °C.

Fig. 4 shows the dependence of mirror loss and interstitial peak suppression on coupling strengths for both symmetric $(\kappa_1 = \kappa_3 \neq \kappa_2)$ and asymmetric $(\kappa_1 = \kappa_2 \neq \kappa_3)$ designs. The interstitial peak suppression for the asymmetric design is better compared to that obtainable with the symmetric coupler designs.

3. Measurement Results

The laser was measured on a temperature controlled stage set at 20 °C. The threshold current is 56 mA. The light–current–voltage (LIV) curve from using an integrating sphere and collecting light outputs from both sides is shown in Fig. 5. The kinks in the curve are due to mode hoping from the changing cavity phase with input current. The output light is coupled into a 2 μm spot-size lensed fiber and used to measure the optical spectrum and linewidth. The wavelength tuning is achieved using three thermal tuners: one each for tuning the CRR mirrors and one for tuning the longitudinal cavity modes.

Fig. 6 shows the coarse tuning of the laser along with the heater powers on each mirror. The side-mode suppression ratio is $>$ 40 dB over the full span. The wavelength of the laser did not

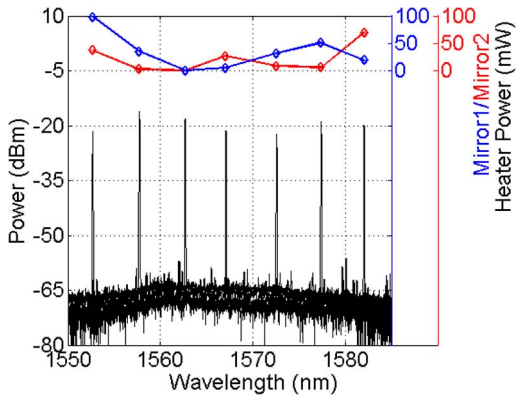

Fig. 6. Coarse tuning of the laser between 1553 nm and 1582 nm.

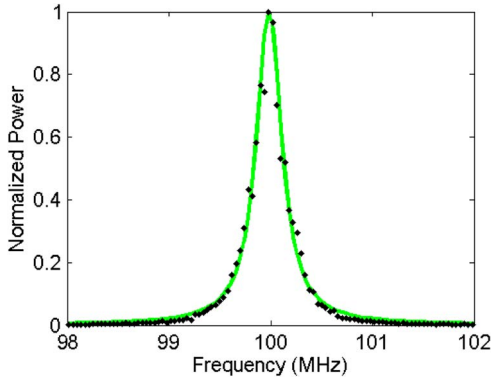

Fig. 7. Self heterodyne linewidth measurement (black dots) and the corresponding Lorentzian fit (green line). The resolution bandwidth is 10 kHz.

trend well with the heaters' input power and we discuss a few possible reasons for this in Section 4. The tuning efficiency of the heater was measured by reverse biasing the SOA and monitoring the photocurrent while sweeping the wavelength of input light into the laser. By recording the change in wavelength of the transmission spectrum with heater power, we calculate the required tuning power for one FSR shift as 91 mW and 103 mW for the 471 μm and 513 μm long rings, respectively. The linewidth of the laser was measured using a delayed self-heterodyne technique using 20 km of single mode large effective area fiber (SM-LEAF). The minimum linewidth measurable with this setup is $\sim$10 kHz. The output power of the laser is amplified using an L-band erbium doped fiber amplifier (EDFA) before sending it to the linewidth measurement setup. The linewidth measured at an input current of 195 mA and no bias on the heaters is 160 kHz, as shown in Fig. 7. The wavelength at this current is 1576.6 nm. The current source was battery powered while measuring the linewidth. The wavelength shift with stage temperature was 0.106 nm/°C in the range of 20 °C to 50 °C. The maximum lasing temperature is 65 °C.

4. Discussion

The key feature of ring resonator based lasers is the effective cavity length enhancement near resonance wavelength. As the wavelength approaches the resonance wavelength, the laser cavity appears longer due to increased photon lifetime in the ring. This is evident in the spacing of the longitudinal modes of the lasing cavity. Fig. 8 shows simulation results for the effective

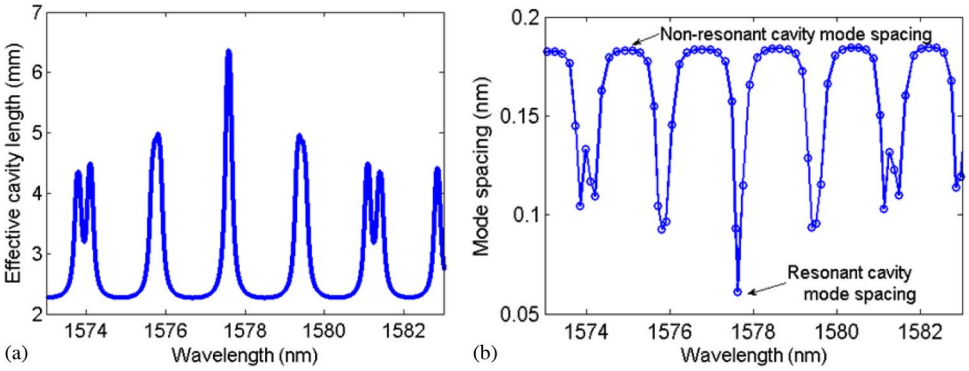

Fig. 8. Simulation results for (a) effective cavity length as a function of wavelength showing almost tripling of length at resonance and (b) location of each longitudinal mode and the spacing from its nearest neighbor, reduced by one third at resonance.

cavity length of the laser and the non uniform spacing of the longitudinal modes. The effective length was observed to be increased by roughly a factor of three. This is due to the large reduction in group velocity at resonance. The locations of the longitudinal modes satisfy the equation $2\beta_a L_a + 2\beta_p L_p + \angle M_1 + \angle M_2 = 2N\pi$, where β_a, β_p, and L_a, L_p are the propagation constants and the lengths of the active and passive sections, respectively. $\angle M_1, \angle M_2$ are the phases acquired by the reflected electric field at the two mirrors. N is an integer. Therefore, one has to be cautious of increasing the cavity Q by making the couplers weak as this might result in multiple longitudinal modes within a resonance peak of the ring to start lasing.

An important observation was made while measuring the linewidth for different SOA bias current. The linewidth decreased from $\sim$5 MHz down to $\sim$200 kHz for a change in current of $\sim$25 mA, and the lowest linewidth occurs just before a mode-hop event. The output power at best increases by a factor of two and cannot explain the factor of 25 in linewidth reduction. Under close inspection, we observe that the change in wavelength with current due to heating is -330 MHz/mA due to rising active region temperature. Over 25 mA this corresponds to a lasing frequency change of $\sim$8 GHz. The spacing between longitudinal modes near resonance is also $\sim$8 GHz measured using a high resolution optical spectrum analyzer (OSA). This confirms the reason for periodic mode hopping every 25–30 mA and the reduced FSR due to resonant length enhancement. Additionally, it also points to the fact that the lowest linewidth occurs on the long wavelength side of the rings resonance. This can be explained using an optical negative feedback effect that occurs when the mirror loss has a steep dependence on wavelength. Fig. 9(a) shows the conversion of frequency fluctuation in a laser to mirror loss fluctuation while lasing on a slope of the transfer function of a resonant structure. When the wavelength of the laser decreases, the mirror reflectivity increases which increases the photon density in the cavity. This reduces the carrier density in the gain section, which, in turn, increases the refractive index through the free carrier plasma effect. The increase in index pulls the wavelength of the laser up causing a negative feedback loop. This negative feedback effect occurs only on the long wavelength side of the ring resonance. This effect is the likely reason for the significant decrease ($> 10\times$) in linewidth in our lasers and also in other laser designs using ring resonators observed by other research groups [1], [4], [13]. The feedback effect is very fast and has a potential for broad band frequency noise reduction. Although detuning the lasing wavelength off-resonance reduces the contribution to linewidth reduction from cavity length enhancement, the improvement from the negative feedback mechanism is much larger and thus provides an overall reduction in linewidth. This could be an important phenomenon that could be exploited in the future for designing integrated narrow linewidth lasers. This was included in the theory formulated by Agarwal *et al.* [14], in the form of a reduction factor "B" associated with the derivative of mirror loss with frequency without the physical explanation.

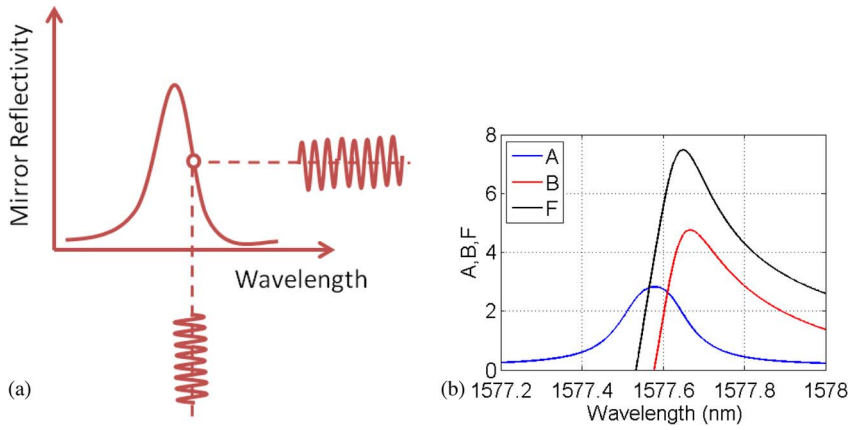

Fig. 9. (a) Diagram showing the conversion of frequency noise to mirror loss fluctuations in a laser with resonant mirrors. (b) Simulated values for parameters *A*, *B*, *F* around resonance wavelength (1577.58 nm) showing large reduction in linewidth ($1/F^2$) on the long wavelength side of the resonance.

Fig. 10. Thermal image of the heater when supplied with 30 mW (4 V), showing non-uniform heating at the hairpin bend in the center due to crosstalk.

Fig. 9(b) shows the simulated values for *A*, *B*, *F* $(= 1 + A + B)$ for our laser using the following expressions [14]:

$$A = \frac{1}{\tau_{\text{in}}} \text{Re}\left\{ i \frac{d}{d\omega} \ln r_{\text{eff}}(\omega) \right\} \tag{1}$$

$$B = \frac{\alpha_H}{\tau_{\text{in}}} \text{Im}\left\{ i \frac{d}{d\omega} \ln r_{\text{eff}}(\omega) \right\} \tag{2}$$

where α_H is the linewidth enhancement factor. $\tau_{\text{in}} = 2n_{\text{eff}}L_a/c$, where n_{eff} and L_a are the effective index and length of the gain section, respectively, and c is the speed of light. $r_{\text{eff}}(\omega)$ is the frequency dependent total reflectivity of the two mirrors.

The linewidth of the laser with the resonant mirrors is given by $\Delta\nu_{\text{ST}}/F^2$ where $\Delta\nu_{\text{ST}}$ is the modified Schawlow-Townes linewidth including the linewidth enhancement factor. The further advantage of this approach is that, there is no appreciable increase in RIN due to conversion of frequency noise to amplitude noise.

A second important note is that the rings for a single mirror are resonantly coupled to each other. Since the couplers are all not identical, the effective ring circumferences are different even if the physical cavity lengths are made the same. This is due to the difference in absolute phase shift acquired along the different coupler lengths. This leads to a resonance splitting and misaligned resonances in a Vernier cavity [15]. Therefore, it is important to have individual tuners to compensate for this error. For full versatile control, the number of tuners required for this laser design is five, two for each mirror and one to tune the longitudinal mode of the laser cavity within the resonance peak, each capable of tuning a full 2π. The tuning map of our laser was also affected by non-uniform heating of the waveguides in each ring of the CRR mirror. Fig. 10 shows the thermal image of the tuners, taken with a commercial thermoreflectance

microscope. The thermal map shows non-uniform heating near the hairpin bends of the tuners. The non-uniform heating and lack of individual tuners on the rings are the reasons for the unpredictable tuning map in our fabricated lasers.

5. Conclusion

In conclusion, we have demonstrated a tunable laser on the heterogeneous silicon platform using coupled ring resonator mirrors. The CRR mirror design does not use a drop port waveguide and preserves the laser power to just two ports and can be reduced to one port if necessary. The resonant mirrors also allow the reduction of optical linewidth using an optical negative feedback mechanism and can be a useful feature for designing future narrow linewidth tunable lasers. The laser demonstrated has an output power $>$ 15 mW and a linewidth of 160 kHz. The coarse tuning range is 29 nm and the side-mode suppression ratio is $>$ 40 dB over the full tuning range. A more predictable tuning map is possible by designing individual heaters on each ring of the CRR mirror and by designing the ring lengths to avoid the resonance splitting and spacing the heaters appropriately to avoid thermal cross talk.

Acknowledgment

The authors would like to thank M. Belt for helping with the linewidth measurement setup, as well as Prof. N. Dagli of UCSB for helpful discussions.

References

[1] K. Sato *et al.,* "High output power and narrow linewidth silicon photonic hybrid ring-filter external cavity wavelength tunable lasers," in *Proc. ECOC*, Sep. 21–25, 2014, pp. 1–3.
[2] P. Evans *et al.,* "Multi-channel coherent PM-QPSK InP transmitter photonic integrated circuit (PIC) operating at 112 Gb/s per wavelength," presented at the Opt. Fiber Commun. Conf./Nat. Fiber Optic Eng. Conf. Opt. Soc. Amer., Los Angeles, CA, USA, Paper PDPC7, 2011.
[3] M. Seimetz, "Laser linewidth limitations for optical systems with high-order modulation employing feed forward digital carrier phase estimation," in *Proc. Opt. Fiber Commun./Nat. Fiber Opt. Eng. Conf.*, Feb. 24–28, 2008, pp. 1–3.
[4] J. Hulme, J. Doylend, and J. Bowers, "Widely tunable Vernier ring laser on hybrid silicon," *Opt. Exp.*, vol. 21, no. 17, pp. 19718–19722, Aug. 2013.
[5] S. Keyvaninia *et al.,* "Demonstration of a heterogeneously integrated III–V/SOI single wavelength tunable laser," *Opt. Exp.*, vol. 21, no. 3, pp. 3784–3792, Feb. 2013.
[6] T. Creazzo *et al.,* "Integrated tunable CMOS laser," *Opt. Exp.*, vol. 21, pp. 28 048–28 053, 2013.
[7] J. Lee *et al.,* "High power and widely tunable Si hybrid external-cavity laser for power efficient Si photonics WDM links," *Opt. Exp.*, vol. 22, no. 7, pp. 7678–7685, Apr. 2014.
[8] B. Liu, A. Shakouri, and J. E. Bowers, "Wide tunable double ring resonator coupled lasers," *IEEE Photon. Technol. Lett.*, vol. 14, no. 5, pp. 600–602, May 2002.
[9] C. Zhang *et al.,* "Low threshold and high speed short cavity distributed feedback hybrid silicon lasers," *Opt. Exp.*, vol. 22, no. 9, pp. 10 202–10 209, May 2014.
[10] Y. Chung, D.-G. Kim, and N. Dagli, "Reflection properties of coupled-ring reflectors," *J. Lightw. Technol.*, vol. 24, no. 4, pp. 1865–1874, Apr. 2006.
[11] O. Schwelb, "Band-limited optical mirrors based on ring resonators: Analysis and design", *J. Lightw. Technol.*, vol. 23, no. 11, pp. 3931–3946, Nov. 2005.
[12] I. Chremmos and O. Schwelb, "Optimization, bandwidth and the effect of loss on the characteristics of the coupled ring reflector," *Opt. Commun.*, vol. 283, no. 18, pp. 3686–3690, Sep. 2010.
[13] P. Dong *et al.,* "Novel integration technique for silicon/III–V hybrid laser," *Opt. Exp.*, vol. 22, no. 22, pp. 26 854–26 861, Nov. 2014.
[14] G. P. Agrawal and C. H. Henry, "Modulation performance of a semiconductor laser coupled to an external high-Q resonator," *IEEE J. Quantum Electron.*, vol. QE-24, no. 2, pp. 134–142, Feb. 1988.
[15] M. Popovic, C. Manolatou, and M. Watts, "Coupling-induced resonance frequency shifts in coupled dielectric multicavity filters," *Opt. Exp.*, vol. 14, no. 3, pp. 1208–1222, Feb. 2006.